creative commons

COMMONS DEED

저작자표시-비영리-변경금지 2.0 대한민국

이용자는 아래의 조건을 따르는 경우에 한하여 자유롭게

- 이 저작물을 복제, 배포, 전송, 전시, 공연 및 방송할 수 있습니다.

다음과 같은 조건을 따라야 합니다:

저작자표시. 귀하는 원저작자를 표시하여야 합니다.

비영리. 귀하는 이 저작물을 영리 목적으로 이용할 수 없습니다.

변경금지. 귀하는 이 저작물을 개작, 변형 또는 가공할 수 없습니다.

- 귀하는, 이 저작물의 재이용이나 배포의 경우, 이 저작물에 적용된 이용허락조건을 명확하게 나타내어야 합니다.
- 저작권자로부터 별도의 허가를 받으면 이러한 조건들은 적용되지 않습니다.

저작권법에 따른 이용자의 권리는 위의 내용에 의하여 영향을 받지 않습니다.

이것은 이용허락규약(Legal Code)을 이해하기 쉽게 요약한 것입니다.

Disclaimer

dCollection

Master of Science in Mechanical Engineering

Design of anti-reflecting metamaterials against inhomogeneous media

비균일한 매질에 대한 무반사 메타물질 설계

August 2023

Graduate School of Mechanical Engineering
Seoul National University

Jae Heung Cho

Design of anti-reflecting metamaterials against inhomogeneous media

Advisor Yoon Young Kim

Submitting a master's thesis of
Mechanical Engineering

April 2023

Graduate School of Mechanical Engineering
Seoul National University

Jae Heung Cho

Confirming the master's thesis written by
Jae Heung Cho

June 2023

Chair	Do Nyun Kim	(Signature)
Vice Chair	Yoon Young Kim	(Signature)
Examiner	Jinkyu Yang	(Signature)

Abstract

Acoustic wave transmission in inhomogeneous media poses a significant challenge in various ultrasonic applications, such as biomedical imaging, treatment, and nondestructive testing. While the time-reversal method with wavefront control has shown promise in enhancing energy transmission to specific regions, it fails to address the inherent impedance mismatch between the inhomogeneous medium and the background medium, leading to undesirable back-scattering reflections.

To overcome this limitation, we present a novel methodology in this paper for designing anti-reflective metamaterials placed in front of the inhomogeneous medium, enabling the transmission of incident energy without reflections. These anti-reflective metamaterials are fabricated as a porous layer with simple holes under a 2D guided wave system, and the positions of these holes are determined through optimization techniques.

We optimize an anti-reflective metamaterial using a genetic algorithm (GA) and assess its performance through numerical simulations. The results demonstrate that the metamaterial effectively suppresses reflections in two distinct systems: one involving rigid obstacles in air and the other with skull obstacles in water. This research offers a promising avenue for enhancing acoustic wave transmission in complex media, contributing to the advancement of ultrasonic applications across various domains.

Keyword : Acoustic waves, Anti-reflection, Metamaterial, Inhomogeneous media, Full transmission, Porous media.

Student Number : 2021-25481

Table of Contents

Chapter 1. Introduction 1

Chapter 2. Theoretical Background 4

Chapter 3. Design Example 15

Chapter 4. Simulation and Result 25

Conclusion 38

Bibliography 40

Abstract in Korean 43

Chapter 1. Introduction

1.1. Study Background

Despite advancements in imaging techniques for opaque media with the progress of measurement technology, ultrasonic remains a prominent choice [1]. This is attributed to its affordability as a surveying method, owing to its low equipment and operational costs. Moreover, its user-friendliness and popularity arise from its ability to provide internal models through straightforward measurement of reflected waves. Additionally, ultrasonic boasts a broad frequency bandwidth and excellent selectivity, enabling precise target modeling and energy concentration within specific regions [2]. Compared to radiation-based methods, ultrasonic exert minimal impact on the target, making it a safe option for nondestructive testing or examinations involving fetuses [3].

However, the efficiency of acoustic measurements is notably diminished when encountering inhomogeneous obstacles, with prominent examples including the human skull and concrete structures [4-5]. These obstacles contain numerous porous holes, causing a significant portion of ultrasonic waves to be reflected. Upon encountering these internal non-uniformly distributed cavities, incident ultrasonic waves experience high impedance differences with the medium, leading to substantial energy scattering. Consequently, the sound waves scattered backward become integrated into the reflected waves, drastically reducing

transmittance. The prevalent non-uniformity in inhomogeneous media primarily arises from such porosity, making it imperative to address this issue to enhance the permeability of inhomogeneous media [6-7].

Over the years, extensive research has investigated acoustic wave transmission in inhomogeneous media. Notably, significant efforts have been made by researchers like Fink, who focused on adjusting the phase of incident waves to attain desired wavefront shapes post-transmission, as well as Heekyung Koh, who utilized AI techniques to enhance image resolution through post-processing [8-9]. However, despite these advancements, prior research has yet to be identified that specifically addresses the reduction of incident wave reflections and aims to enhance the overall transmittance.

1.2. Purpose of Research

This study endeavors to eradicate the reflections of incident waves within a system that penetrates an inhomogeneous medium, facilitating the complete penetration of all energy through the obstacle. Significantly expanding the subject studied in electromagnetism to the realm of acoustics, we introduce a novel approach of utilizing an equally inhomogeneous layer, known as the meta-layer, strategically placed ahead of the inhomogeneous medium. Through carefully designs achieved via optimization techniques, our simulations demonstrate the effective elimination of wave reflections, enabling high transmittance for all incident wave

modes in both system types. Furthermore, we briefly explore potential avenues for future research and the developmental prospects of anti-reflection metamaterials, affirming their promising applications in forthcoming studies.

Chapter 2. Theoretical Background

2.1. Metamaterial

This research chose metamaterials to enhance inhomogeneous obstacles' energy propagation efficiency. Metamaterials refer to materials exhibiting effective physical properties at specific frequencies due to their artificially designed structural characteristics [10]. Incident waves can be systematically molded to possess predetermined directions and magnitudes as vectors by appropriately configuring or shaping these designed structures. Although metamaterials consist of conventional materials in a composite arrangement, when treated as a unified entity and observed collectively, they exhibit extraordinary behaviors, such as showcasing negative mass or stiffness.

Metamaterials have garnered significant attention due to their remarkable wave manipulation capabilities, positioning them as potential breakthroughs in overcoming physical limitations in various wave-related fields, including optics, electromagnetics, acoustics, and elastic waves. Ongoing research in these domains actively explores the utilization of metamaterials [11-12]. Notably, investigations have been conducted to enhance usability through bandwidth manipulation of wave transmission frequencies, object cloaking, wavefront control, and hyperlens (refer to Fig. 2.1) [13-15]. Specifically, in this study, we will harness metamaterials' mode conversion and reflection matrix matching capabilities [16-17].

In our study, we will introduce an anti-reflection meta-layer harnessing the unique properties of metamaterials. The meta-layer is derived from metamaterials and is characterized by the repetition of specific structures, allowing for changes in effective properties with only one or a few layers [18-19]. Unlike conventional inhomogeneous layers, which typically reflect a significant portion of incident waves, the meta-layer offers improved transmission efficiency. To address the issue of reflections and to ensure the complete transmission of energy, we will incorporate an optimized anti-reflection meta-layer ahead of the obstacle layers (refer to Fig. 2.2). This novel approach aims to mitigate reflection-related challenges and enhance the overall energy propagation efficiency through the use of tailored meta-materials.

2.2. 2D guided wave system

In contrast to general acoustic wave systems, which often employ 1D simulations for computational efficiency, our study conducted simulations in 2D guided wave systems [20]. The choice of a 2D system is essential due to the influence of inhomogeneity caused by porosity, which is determined by the position and radius of the hole [21]. In this research, it is crucial to consider that the incident wave may consist of several mode components, unlike in 1D transmission systems. By setting the reflectance to zero for all modes, the entire wave can be perceived as transmitting all energy,

which forms an essential aspect of our analysis [22−23].

In the 2D guided wave system, the wave number of the incident wave is determined by the physical properties and frequency of the medium. The wave number is represented by a vector with components along the x−axis, which represents the direction the wave propagates, and the y−axis, which is perpendicular to the direction of propagation, and the propagation of the wave depends on the ratio of these components. Notably, the wave number in the y−axis direction can only take half−wave multiples values, given the boundary condition of a hard wall. This constraint arises from the requirement that the wave's displacement at the wall must be zero for a hard wall boundary condition. As a result, the y−axis wave number for propagating waves only assumes specific non−continuous values, known as wave modes [24]. The wave mode is generally defined as 0 when the value of the wave number in the y−axis direction is 0 and as 1 when it equals half of a wavelength. Subsequently, the mode value increases with each subsequent half−wavelength increment.

Moreover, suppose the value of the wave number in the y−axis direction surpasses the absolute value of the total wave number. In that case, the wave exhibits a non−propagating characteristic, rendering it unable to transmit energy. By adjusting the length of the y−axis in the system, we can effectively control the number of modes that can be generated. Manipulating the system's y−axis length provides a means to regulate the wave's behavior and determine the feasibility of specific modes, thereby offering a valuable means of

controlling wave propagation and energy transmission in the system.

This study employs the scattering matrix concept to determine the transmittance and reflectance of waves [25]. The scattering matrix organizes the transmittance and reflectance based on the incident direction of the wave into a single matrix. It contains components representing both sides' incident direction, transmittance, and reflectance. In a 1D system, the scattering matrix takes a scalar value for each component. However, in the 2D guided wave system, where multiple modes can occur even with a single incident mode, the transmittance and reflectance are represented as $n \times n$ matrices, where n corresponds to the number of modes. Consequently, the scattering matrix in the 2D guided wave system adopts a $2n \times 2n$ matrix format to accommodate the multiple modes effectively. Consequently, for forward transmission matrix $\mathbf{t}$, forward reflection matrix $\mathbf{r}$, backward transmission matrix $\mathbf{t}'$, and backward reflection matrix $\mathbf{r}'$, the scattering matrix, $\mathbf{S}$, can be defined as:

$$\mathbf{S} = \begin{pmatrix} \mathbf{r} & \mathbf{t}' \\ \mathbf{t} & \mathbf{r}' \end{pmatrix} \tag{2.1}$$

Indeed, the transmission component of the scattering matrix provides crucial insights into whether the wave is entirely transmitted. Even if the incident wave is composed of a single mode component, it transforms into a combination of various modes as it propagates through the obstacle. By examining the energy of each mode in the transmitted wave and ensuring that they are all equal to the mode energy of the incident wave, we can conclude that the wave has been transmitted without any loss. This method enables a

comprehensive assessment of the wave's behavior and energy conservation during transmission, allowing us to evaluate the effectiveness of our anti-reflection meta-layer design in achieving efficient and lossless wave propagation through inhomogeneous media.

2.3. Formula derivation

The proposed methodology to achieve non-reflection involves adding an inhomogeneous obstacle layer, comprising identically configured holes, in front of the inhomogeneous obstacle with randomly distributed holes, as illustrated in Fig. 2.3. The objective is to enable the transmission of all incident waves from the left without any reflections. To attain this goal, we will design the left-side design layer to complement the right-side obstacle layer. This design approach has been extensively explored in electromagnetism and is now being adapted and expanded to the field of acoustics in this study [25]. The formulation is based on the theoretical foundation in Michael Horodynsk's electromagnetism thesis, which serves as the fundamental basis for this investigation. By leveraging this well-established theoretical framework, we aim to establish a novel application of the design methodology in acoustics to achieve efficient wave transmission in inhomogeneous media.

Without energy consumption, such as absorption in the system, the scattering matrix adheres to flux conservation principles. In this

situation, the total energy of the incident wave remains conserved throughout the scattering process, leading to the equivalence of energy flux before and after scattering. The scattering matrix effectively describes the transformation of wave amplitudes and directions while preserving energy, ensuring that the total energy of the incident wave is equal to the combined energy of the transmitted and reflected waves. In this case, the scattering matrix S has the relation:

$$\mathrm{S}^{\dagger}\mathrm{S} = \mathrm{S}\mathrm{S}^{\dagger} = \mathbb{I} \tag{2.2}$$

where symbol † denoted conjugate transpose, $\mathbb{I}$ denoted identity matrix. In this study, we define the scattering matrix of the design matrix as $\mathrm{S_L}$ and the scattering matrix of the obstacle layer as $\mathrm{S_R}$, as illustrated in Fig. 2.4. Assuming that the wave travels from left to right in the system, the system's total transmission matrix T and reflection matrix R can be expressed in the form of an infinite geometrical series. Combining the elements above, we arrive at the following outcome:

$$\mathrm{T} = \mathrm{t_R}(\mathbb{I} - \mathrm{r_L}'\mathrm{r_R})^{-1}\mathrm{t_L} \tag{2.3a}$$

$$\mathrm{R} = \mathrm{r_L} + \mathrm{t_L}'\mathrm{r_R}(\mathbb{I} - \mathrm{r_R}\mathrm{r_L}')^{2}\mathrm{t_L} \tag{2.3b}$$

By implementing energy conservation to the scattering matrix within the design matrix, we can derive the subsequent equation from the expressions presented in Eqs. (2.1) and (2).

$$\mathrm{S_L}\mathrm{S_L}^{\dagger} = \begin{pmatrix} \mathrm{r_L} & \mathrm{t_L}' \\ \mathrm{t_L} & \mathrm{r_L}' \end{pmatrix}\begin{pmatrix} \mathrm{r_L} & \mathrm{t_L}' \\ \mathrm{t_L} & \mathrm{r_L}' \end{pmatrix}^{\dagger} = \begin{pmatrix} \mathbb{I} & 0 \\ 0 & \mathbb{I} \end{pmatrix} \tag{2.4}$$

The expression below emerges from the intersection of the first row and second column within the resultant matrix:

$$\mathrm{r_L t_L^\dagger} + \mathrm{t'_L r'^\dagger_L} = 0 \tag{2.5}$$

where $\mathbf{0}$ denoted zero matrix. Upon incorporating the equations represented as Eqs. (2.5) and taking into account the assumptions specified in Eqs. (2.6) into the context of Eqs. (2.3b) yields surprising results.

$$\mathrm{r'^\dagger_L} = \mathrm{r_R} \tag{2.6}$$

$$\mathrm{R} = r_L + t'_L r_R (\mathbb{1} - r_R r'_L)^2 t_L = 0 \tag{2.7}$$

In this case, it becomes apparent that the complete reflection matrix, denoted as R, becomes entirely null within the system, leading to the comprehensive transmission of all waves. The previously mentioned expression equates to the subsequent form:

$$\mathrm{T^\dagger T} = \mathrm{T T^\dagger} = \mathbb{1} \tag{2.8}$$

As the conditions specified in Eqs. (2.8) are met; this particular state ensures the absence of reflections and signifies that every incident wave is effectively conveyed without experiencing loss.

From these findings, we have theoretically devised a system where waves can penetrate all potential incident modes in the acoustic system. Remarkably, the outcomes do not necessitate any information regarding the structure or transmittance of the barrier layer. During the derivation and optimization of the equation, the transmission matrix played a central role. However, in the actual manufacturing of the metamaterial, the design layer can be constructed exclusively using components of the reflection matrix. This aspect simplifies the practical implementation of the anti-reflection meta-layer, offering a promising avenue for achieving efficient wave transmission in real-world applications.

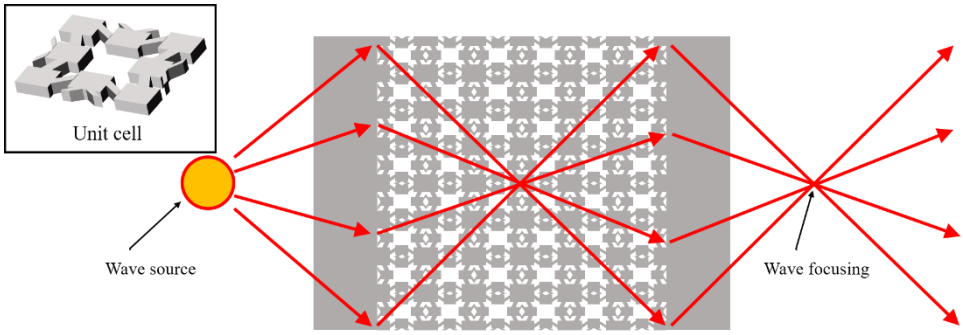

Fig. 2.1. A metamaterial with wave focusing function proposed by J. H. Oh. General materials are engineered to possess distinct physical properties by utilizing unit cells with identical structures.

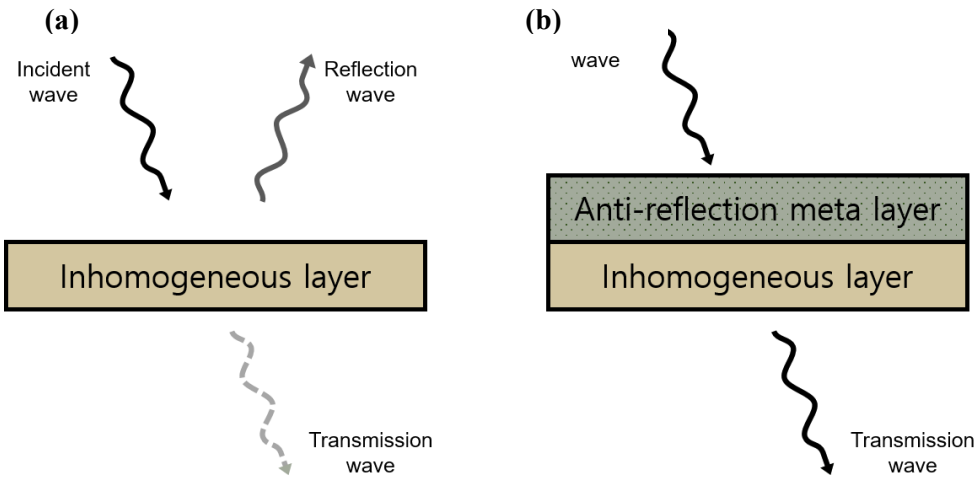

Fig. 2.2. The meta-layer diagram. (a) A general inhomogeneous layer reflects most of the incident wave. (b) However, a properly designed anti-reflection meta-layer is placed before the inhomogeneous layer to achieve anti-reflection and complete transmission.

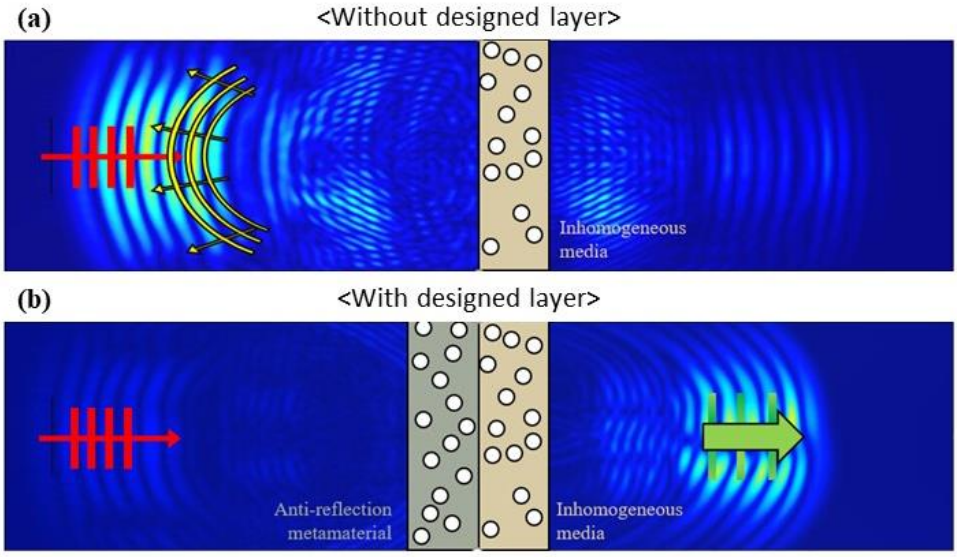

Fig. 2.3. The simulation depicts the behavior of waves encountering inhomogeneous media. (a) Most waves encounter an inhomogeneous obstacle layer and are reflected. (b) Anti-reflection is achieved by adding an adequately designed anti-reflecting layer to the front surface.

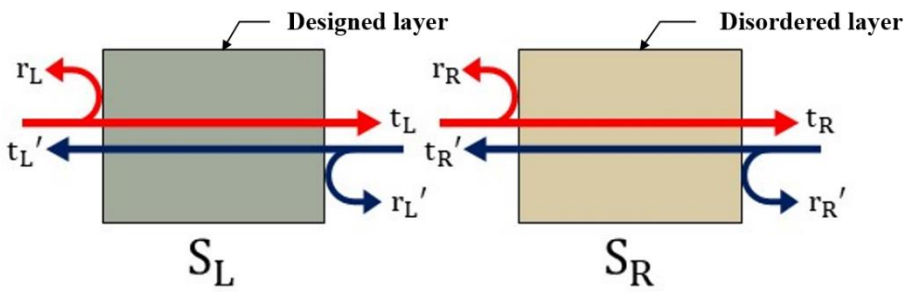

Fig. 2.4. The illustration demonstrates the concept of formula derivation. A designed layer (S_L) is added to the disordered medium (S_R) to achieve anti-reflection for the incident wave.

Chapter 3. Design Example

3.1. System modeling process

In this phase, our simulation involves modeling an inhomogeneous medium using porous obstacles based on insights from various related papers [5-6]. The inhomogeneous medium will be represented by simulating the cross-section of the skull, which serves as a representative example of such media. We aim to validate the theoretical concepts through simulations within a system encompassing four modes. The configuration of the system's mode is represented by the waveform, which can be described using the subsequent equation.

n is even: $$A(y) = \cos(n\pi y/W) \tag{3.1a}$$

n is odd : $$A(y) = \sin(n\pi y/W) \tag{3.1b}$$

where n denotes the specific mode, y refers to the vertical position along the y-axis of the system, and W corresponds to the vertical extent of the system along the y-axis. The amplitude of the wave, denoted as $A(y)$, is a function dependent on the vertical position y within the system. As previously noted, the wave exhibits a null value at the boundary.

Firstly, we will conduct simulations for a simple case, where the medium is air, and the scatter consists of a rigid body. This preliminary step aims to demonstrate non-reflection in a heterogeneous system composed of water and the skull, thereby determining its suitability for real-world applications. Throughout

both simulations, we assume that the wave passes through the medium without attenuation due to interaction with the scatter. This foundational exploration will confirm the effectiveness and applicability of the proposed anti-reflection methodology in modeling that closely mimic actual conditions.

Using air as the foundational medium, we embark on a straightforward simulation arrangement to evaluate the practical viability of achieving anti-reflection effects. This arrangement is achieved by introducing an additional inhomogeneous layer, with a length denoted as l, ahead of a parallel inhomogeneous layer of equal length. Employing a relatively low frequency of 10 kHz (f), we establish the inhomogeneous medium by strategically placing rigid scatters, each with an identical radius r, at random positions within the medium.

In this system, a wave is incident from the left side, traversing through the air with a density represented as ρ_0 and a speed of sound denoted as c_0. The system, with a total length of L, accommodates the propagation of the wave. The extent of the system, characterized by its thickness W, limits the highest achievable mode within the system. However, this mode is eventually perturbed by interactions with the rigid scatters, leading to a disordered scattering pattern that spans the entire system.

To deal with this scattering phenomenon, we now optimize the positioning of identical rigid scatters within the system while keeping their radius and count consistent. The objective is to achieve an anti-reflection effect within this configuration, as illustrated in Fig 3.1 (a).

This initial simulation demonstrates the pragmatic feasibility of the anti-reflection concept, thereby establishing a groundwork for subsequent investigations involving more intricate and representative systems.

Multiple porous cavities induce wave scattering and diffused wave reflections in the system where the skull functions as the foundational medium. To simulate this situation, we introduce a distribution of water-filled voids within a medium with the same material properties as the skull. These voids are randomly positioned and are assigned varying radii, following a normal distribution characterized by a mean radius μ and a variance σ.

Upon the incidence of a wave from the left side, it initially travels through the water medium characterized by a density ρ_w and a speed of sound denoted as c_w. As the wave penetrates the skull medium, which possesses a density ρ_s and a speed of sound c_s, a portion of the wave is reflected. It further complicates matters; waves that manage to enter the skull medium encounter water-filled voids within the structure. This interaction results in subsequent reflections and refractions, contributing to the emergence of intricate scattering patterns.

In due course, these waves continue to propagate, eventually returning to the water medium and giving rise to additional reflections. The entire system operates at a specific frequency denoted as a value commonly employed in medical ultrasound applications. A detailed depiction of the system configuration is provided in Fig 3.1 (b).

To mitigate these reflections, we will optimize the system to achieve zero energy reflectance by introducing a skull layer with a constant radius r and an equal number of water-filled holes on the front side. By carefully designing this configuration, we aim to demonstrate the capability of the anti-reflection meta-layer in reducing reflections and facilitating more efficient wave propagation through the inhomogeneous medium. This investigation will contribute to validating the practical applicability of the proposed methodology in overcoming the challenges posed by inhomogeneous media and realizing efficient wave transmission.

Both systems, referring to the case with air as the base medium and the case with the skull as the base medium, include 20 scatters in each designed layer and each obstacle layer. More detailed information can be found in the Table. 3.1-2, which presents comprehensive details regarding the physical values used in the simulation.

3.2. Optimization process

The optimization and simulation were conducted using the genetic algorithm (GA) optimization technique, employing Comsol and Matlab. In each case, a disordered layer with a specific distribution was placed on the right side, and a layer of the same thickness was added to the left side, designated as the design layer. The goal was to optimize the x and y positions of the scatters within

the design layer to achieve the desired target characteristics. As a result, there were 40 design variables, twice the number of scatters in the system. The optimization process utilized GA with the following cost function C:

$$C = 1 - \sum_i \left|\mathrm{T}^\dagger \mathrm{T}\right|_{ii} \tag{3.2}$$

The objective of this cost function was to attain the best result when the $\mathrm{T}^\dagger\mathrm{T}$ matrix has the value of the identity matrix. By optimizing the design variables using GA and the given cost function, the system is fine-tuned to achieve the desired outcome, where the $\mathrm{T}^\dagger\mathrm{T}$ matrix closely resembles the identity matrix. This successful outcome validates the effectiveness of the proposed anti-reflection meta-layer in significantly reducing reflections and optimizing wave transmission through inhomogeneous media.

The Genetic Algorithm (GA) is a technique that optimizes design variables by generating multiple groups with random values and refining them through various processes, as shown in Fig 3.2. In each generation, the algorithm evaluates the fitness of each group based on the cost function, selecting the best group of variables that yields optimal results. It then preserves the traits of these good groups, exchanges some of the variables with other groups to promote diversity, and gradually introduces mutations to improve the results.

For this study, 40 design variables were utilized, and the two groups that produced the best results were preserved as excellent traits. The exchange rate between groups was 20%, allowing for a balanced mix of diverse traits. Additionally, mutations were

introduced to 75% of the variables in each generation, gradually enhancing the overall performance by exploring new possibilities and avoiding getting stuck in local optima.

The optimization process was effectively guided by employing the GA with these settings to converge toward the best possible solution. This solution resulted in the successful design and validation of the anti-reflection meta-layer for efficient wave transmission in inhomogeneous media.

Table. 3.1. Geometrical and physical properties, variables used in the air system.

Design Variables	Symbol	Values
Density $(\mathbf{kg}/\boldsymbol{m}^3)$	ρ_0	1.225
Speed of sound $(\boldsymbol{m}/\boldsymbol{s})$	c_0	343
Length of system (**cm**)	L	140
Height of system (**cm**)	W	64
Frequency (**kHz**)	f	10
Length of layer (**cm**)	l	50
Number of holes		20
Radius of hole (**cm**)	r	3.2

Table. 3.2. Geometrical and physical properties, variables used in the WSW system.

Design Variables	Symbol	Values
Density of water (**kg/m^3**)	ρ_w	998
Speed of sound in water (**m/s**)	c_w	1440
Density of skull (**kg/m^3**)	ρ_S	1800
Elastic modulus of skull (**GPa**)	E_s	19.7
Length of system (**mm**)	L	500
Height of system (**mm**)	W	28.6
Frequency (**kHz**)	f	100
Length of layer (**mm**)	l	30
Number of holes		20
Radius of match layer hole (**mm**)	r	0.9
Mean radius of obstruction (**mm**)	μ	0.85
Dispersion of obstruction (**mm^2**)	σ	0.15

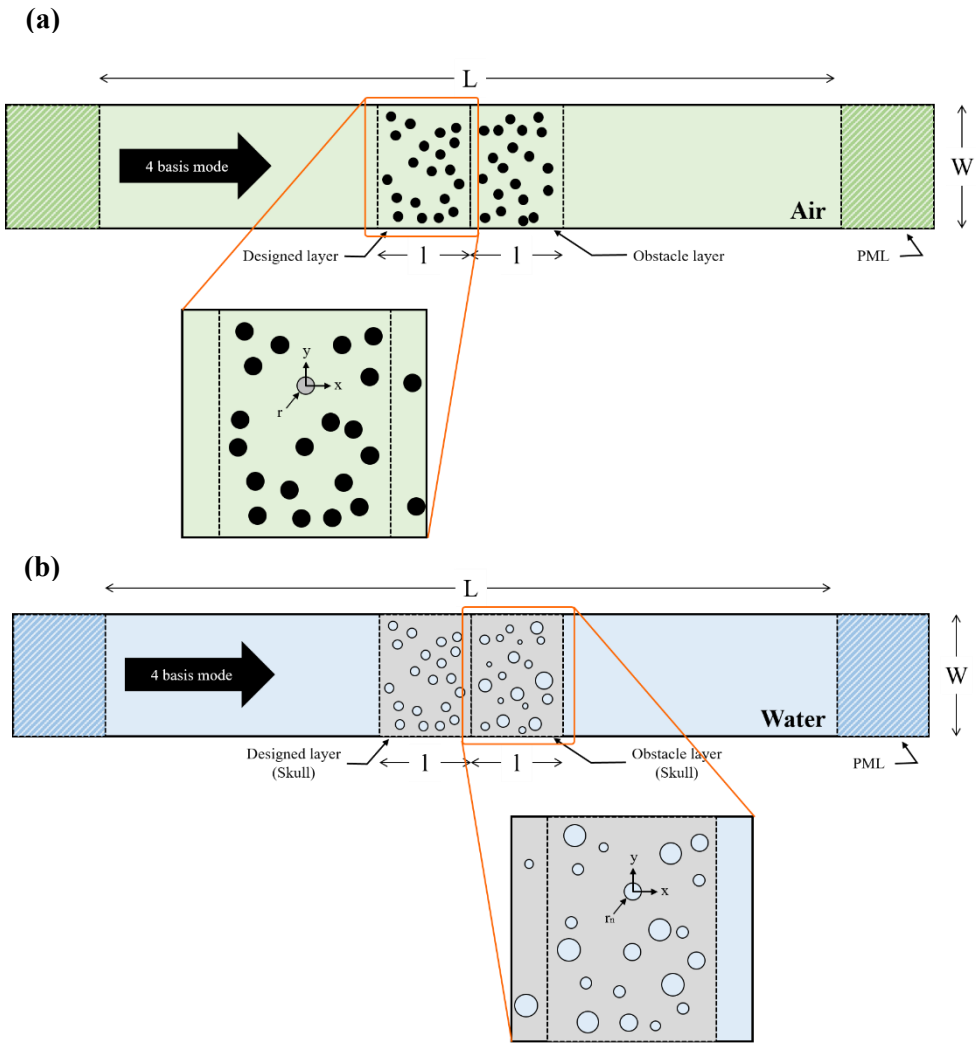

Fig. 3.1. A simple conceptual diagram of the two systems is presented below. The system includes a hard boundary, and Perfectly Matched Layer (PML) is placed on the front and back to suppress reflection. Both the design layer and the obstacle layer consist of 20 scatters. (a) Conceptual diagram of a system using rigid scatter with air as the medium. The wave propagates only through the air and scatters when encountering rigid scatter. (b) Conceptual diagram of the system using water as the medium and the skull as an obstacle. Waves passing through the water traverse the designed and obstacle layers composed of skulls. The scatter in the design layer has the same radius, while the obstacle layer has a random radius following a normal distribution.

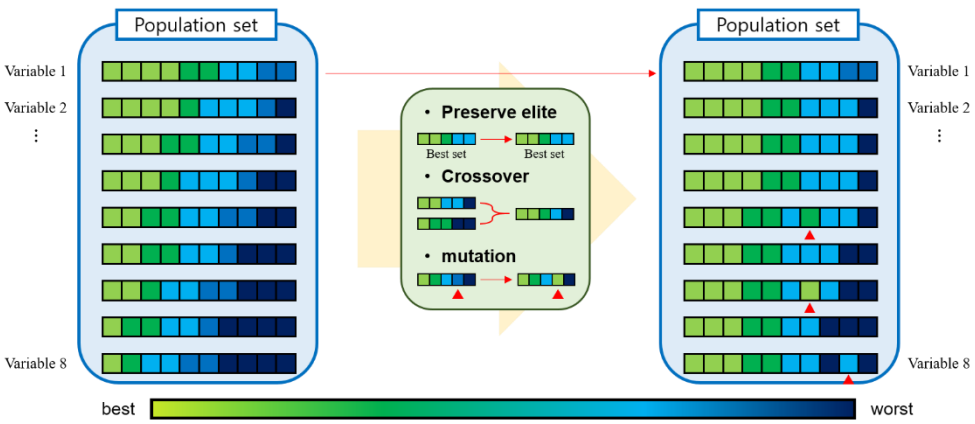

Fig. 3.2. The schematic illustrates the GA (Genetic Algorithm) optimization process. It is an evolutionary optimization technique that iteratively improves solutions through elite conservation, a crossover between variable sets, and mutation of specific variables in a population set composed of random variables.

Chapter 4. Simulation and Result

4.1. Optimization results in an air system

The optimization results for the case with air as the base medium are presented in Fig. 4.1. As shown, the average transmittance of the system with only the existing barrier layer was 69%. However, when the optimized layer was added to the front, the average transmittance significantly improved to 97%. This remarkable enhancement in wave transmission is evident in Fig. 4.2, where the addition of design layers for all four modes in the system resulted in a dramatic disappearance of the reflected wave.

In particular, mode #1 exhibited the highest reflectance after optimization, but even in this case, the reflectance was only 4%. An energy transmittance of over 99% can be achieved by continuing the optimization process through further iterations. This simple yet impactful example effectively demonstrates the successful application of our theoretical background, confirming the accuracy and efficacy of the proposed anti-reflection meta-layer design methodology in improving wave transmission efficiency through inhomogeneous media.

4.2. Optimization results in water-skull-water system

Optimization was carried out in the water-skull-water system (WSW system) to obtain simulation results that could be practically

applied. A critical distinction between this simulation and the one in the air medium lies in the behavior of the last mode (mode #3). Unlike the air medium, waves do not penetrate the skull in the last mode due to the significant difference in the physical properties of the skull and water. Specifically, the wave number of the skull is smaller at the same frequency, causing the propagation mode in water to be unable to propagate through the skull.

This simulation examines the average transmittance of the previous three modes since the last mode exhibits different behavior. By analyzing the transmittance of the first three modes, we can evaluate the overall effectiveness of the anti-reflection meta-layer in facilitating wave transmission through the WSW system. This analysis will provide valuable insights into the practical application of the proposed design methodology in real-world examples involving inhomogeneous media.

The simulation results for position optimization are displayed in Fig. 4.3. As indicated in Fig. 4.4, the average transmittance of the existing obstacle layer is only 35% due to significant hindrance in wave propagation caused by reflections between different materials, unlike the case with air. However, by strategically placing the design layer in front through optimization, the average transmittance increases to more than 90%, even after accounting for energy loss during material penetration.

Notably, mode #2, in the case of a system with only existing obstacles, exhibited a low transmission efficiency of 21%. However, incorporating design layers can dramatically increase the

transmission rate to 98%, significantly improving wave propagation efficiency. These results demonstrate the effectiveness of the anti-reflection meta-layer in overcoming the challenges posed by inhomogeneous media and enhancing wave transmission performance, especially in scenarios where reflections and differences hinder the propagation of waves in material properties.

4.3. Wavefront control

Moreover, the transmission waveform can be finely adjusted based on the obtained transmission matrix. Using the inverse matrix of the transmission matrix makes it possible to mathematically invert the phase of the desired transmitted wave, thereby accurately determining the mode ratio of the incident wave. Fig. 4.5 illustrates that "wavefront control," where the transmitted wave is precisely managed, can be achieved by appropriately adjusting the size and phase of the modes comprising the incident wave.

As depicted in Fig. 4.5, wave focusing is successfully achieved by concentrating the transmitted wave energy into a specific area. This result is accomplished by skillfully combining incident waves with a ratio of 0.35 for mode #0 and 0.65 for mode #2. The resulting fine-tuned wavefront control offers promising opportunities for applications requiring precise targeting and concentration of transmitted wave energy. This capability holds substantial potential for various fields, including biomedical imaging, nondestructive testing, and other ultrasonic applications where controlled wave

propagation is essential for improved performance and accurate results.

4.4. Discussion on optimization cost reduction

We can now discuss the research development direction based on the results and findings obtained in this study. Examining the optimization process, as shown in Fig. 4.6, we observe that GA optimization was utilized. The graph illustrates the optimization process for both types of media. The cost value decreases rapidly up to the initial 100 iterations, but the optimization speed gradually slows down.

This outcome is attributed to the nature of GA optimization, which relies on combining each variable and utilizing mutation to achieve better values. Consequently, it can quickly achieve relatively modest results, such as a transmittance level of 90%. However, obtaining more stringent results, such as a transmittance of 97% or higher, relies more heavily on chance, and as the target transmittance is set higher, the time required for optimization increases exponentially.

As a result, it is worthwhile to consider a combination of approaches for optimization. One possibility is to use GA optimization up to a certain level to attain a satisfactory result quickly and then employ another optimization process, such as the gradient method, to enhance the transmittance further and achieve even higher performance levels. This hybrid approach can leverage both

optimization techniques' strengths and expedite achieving desired high transmittance levels.

4.5. Robustness of system

To verify the robustness of the experimental results, the transmittance in a range beyond the target frequency, known as the bandgap, was measured. Fig. 4.7 (a) displays the results, revealing that the methodology is susceptible to variations in frequency. In a simple system using air, the energy transmittance was measured up to about 15% of the target frequency (10 kHz). At the exact frequency of 10 kHz, the transmittance reached 97%. However, even with a slight difference of only 3% from the target frequency, the transmittance decreased significantly to about 70%.

This behavior is typical in meta-layers and similar structures, where the bandgap's width becomes crucial. A more complex cost function can address this issue and achieve better performance over a wider frequency range [19]. It is essential to consider the trade-offs and design constraints when optimizing the meta-layer for different frequency bands.

Interestingly, a phenomenon is observed where the transmittance recovers as the frequency is further decreased. This result occurs because the scattering is less affected at lower frequencies. However, higher-frequency ultrasound is typically necessary for applications requiring high-resolution ultrasound imaging. Consequently, a target frequency for optimization is a essential approach to achieving the intended purpose and desired

performance in ultrasound applications.

Similarly, the transmittance and positional sensitivity of the scatter in the obstacle layer were examined. In a simple system using air, with the design layers remaining constant, the efficiency was observed when the scatter in the obstacle layer was subject to a random error following the normal distribution. As the range of the distribution increased, the efficiency dropped rapidly. For instance, at a standard deviation of 2 cm, the transmittance decreased to 50%.

This sensitivity analysis, illustrated in Fig. 4.7 (b), emphasizes the importance of creating a well-controlled environment for the practical application of the methodology in real-world situations. To achieve high and consistent transmittance, it is crucial to accurately position the scatters in the obstacle layer and maintain precise control over the system's parameters.

In conclusion, the study's findings underscore the need for meticulous attention to experimental conditions and design precision when implementing the anti-reflection meta-layer approach in real applications. A well-controlled environment will ensure reliable and optimal wave transmission performance through inhomogeneous media, enhancing the methodology's practical applicability in various fields, including biomedical imaging, nondestructive testing, and other ultrasonic applications.

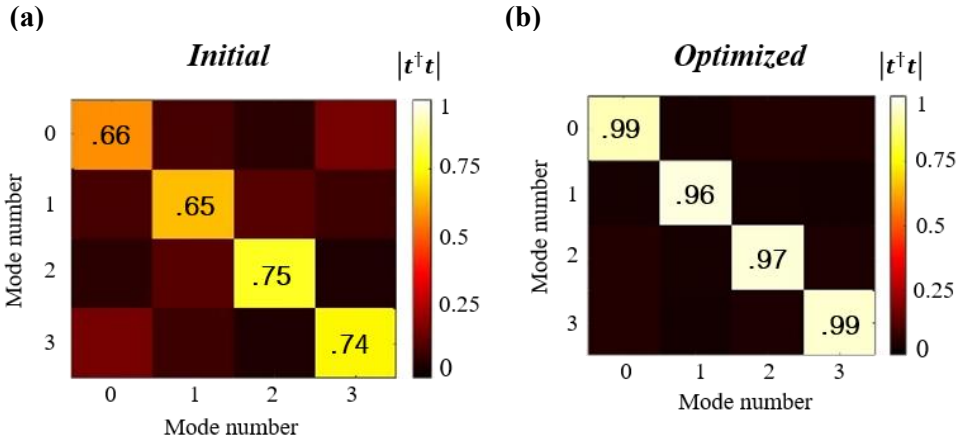

Fig. 4.1. Simulation results of achieving ultrasonic anti-reflection in air medium. (a) Graph of the absolute value of the matrix in the case of only the disturbing layer. (b) Absolute value graph of the matrix when the optimized design layer is added. After installing the design layer, the matrix shows the identity matrix form.

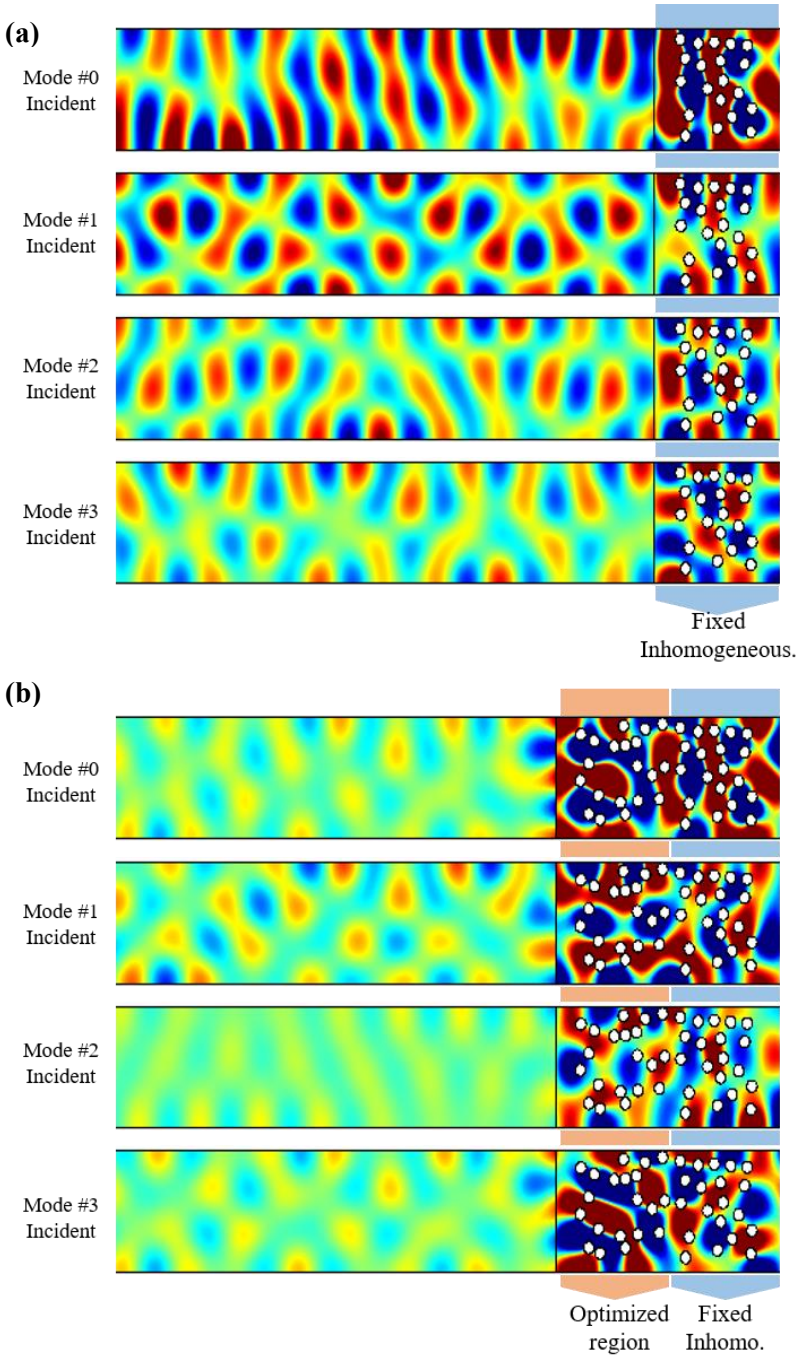

Fig. 4.2. A graph to check the reflected wave of the wave in the air system. (a) Reflected wave when there is only an interfering layer. (b) Reflected wave when a designed layer is added. It can be seen that the reflection is greatly suppressed compared to the previous graph.

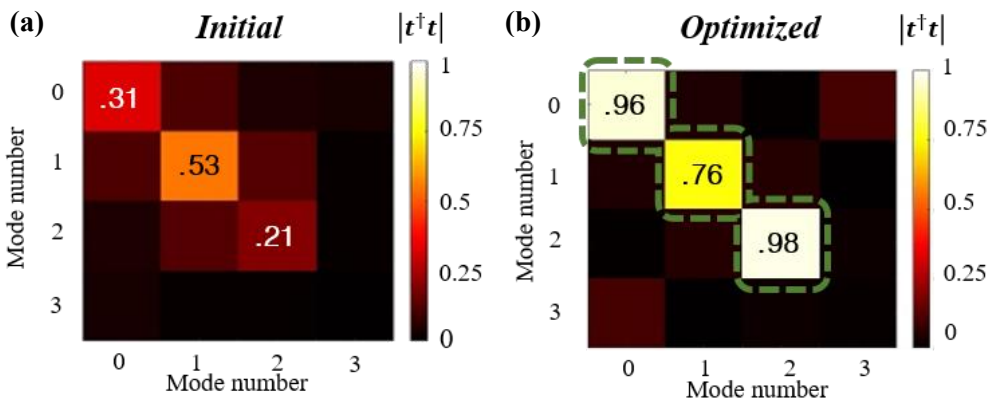

Fig. 4.3. Simulation results of achieving ultrasonic anti-reflection in a WSW medium. (a) Graph of the absolute value of the matrix in the case of only the disturbing layer. (b) Absolute value graph of the matrix when the optimized design layer is added. The transmittance of the mode #2 increased significantly.

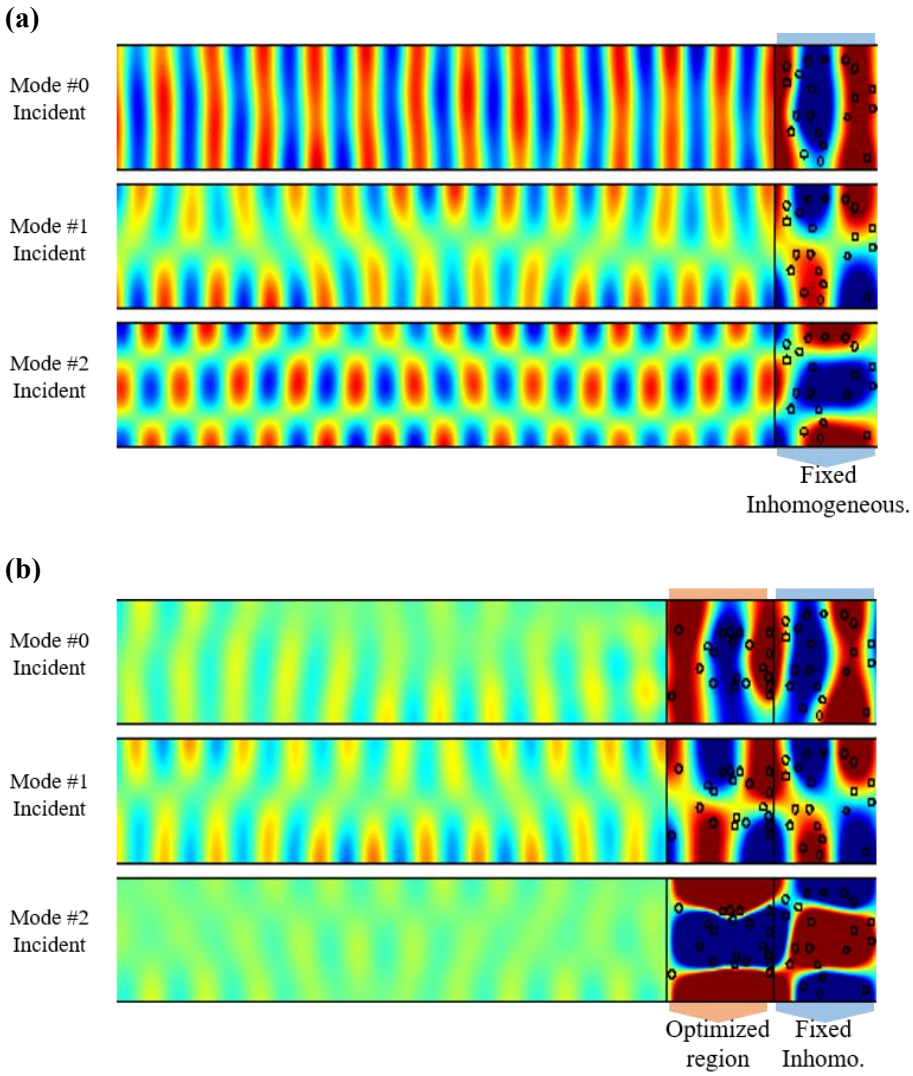

Fig. 4.4. A graph confirming the reflected wave of a wave in a WSW system. (a) Reflected wave when there is only an interfering layer. (b) Reflected wave when a designed layer is added. It can be seen that the reflection is significantly suppressed compared to the previous graph.

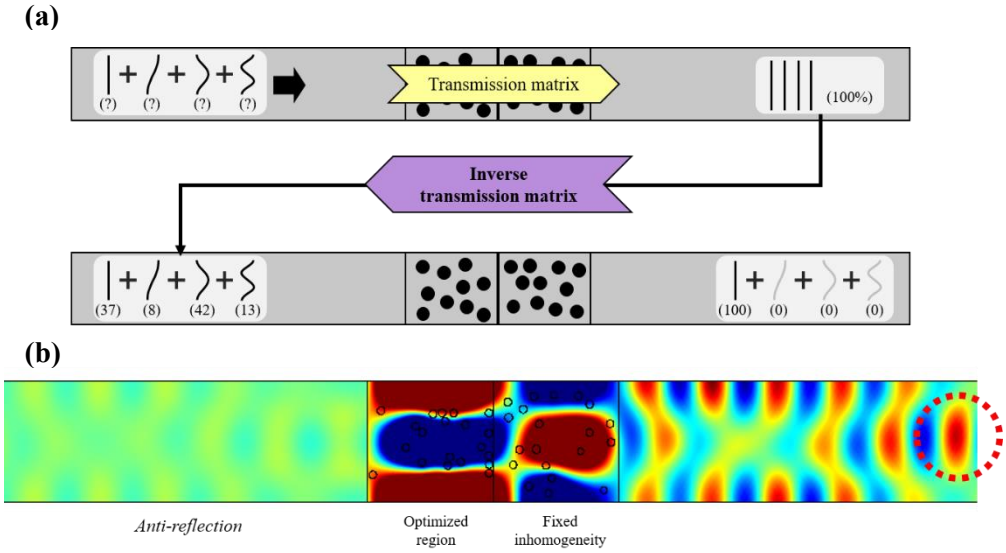

Fig. 4.5. Wavefront control simulation and result. (a) Schematic showing the process of achieving wavefront control. By calculating the waveform of the transmitted wave through an inverse matrix, the mode ratio of the incident wave can be determined. (b) A graph demonstrating wave focusing achieved by adjusting the mode ratio of the incident wave. While suppressing the reflection of waves, all the energy was focused on a specific point.

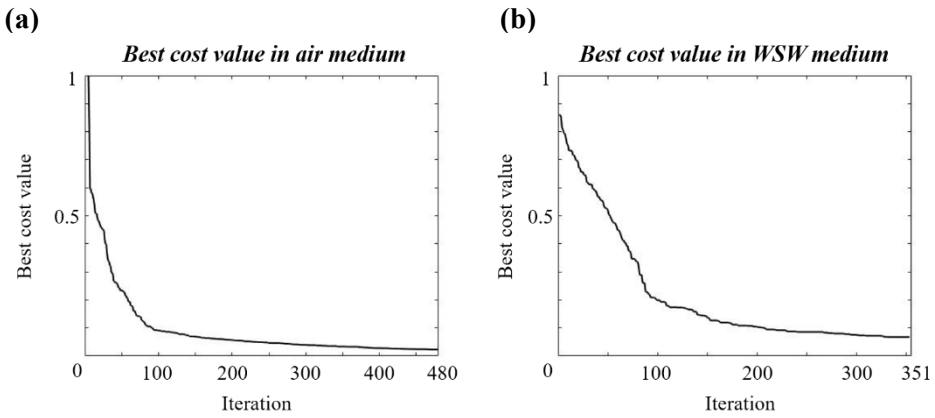

Fig. 4.6. Simulation iteration graph. (a) Optimized cost value graph according to iteration in air medium. (b) Optimized cost value graph according to iteration in WSW medium.

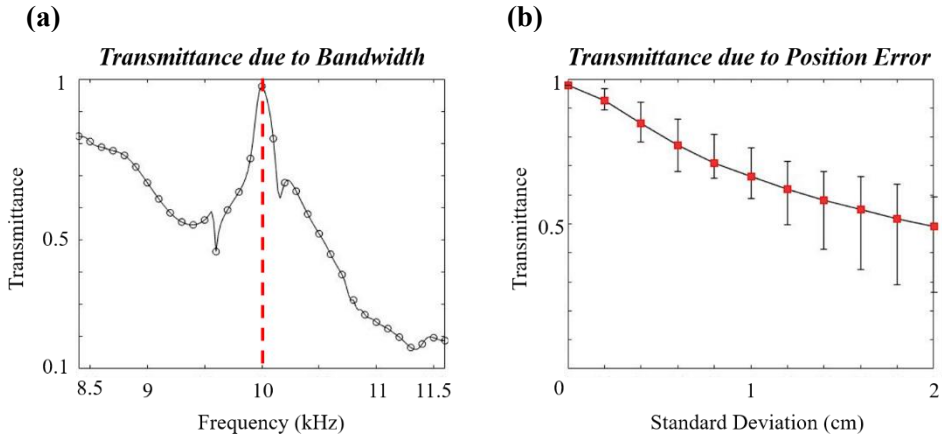

Fig. 4.7. A graph to check the robustness of the system. (a) Transmittance according to frequency. The transmittance is at its maximum at the target frequency and gradually decreases as the distance from it increases. (b) Transmittance according to scatter position error. The transmittance decreases proportionally as the scatter moves away from the exact position.

Conclusion

This study presents a novel design methodology for complete wave transmission without any reflections. By introducing a specially designed porous layer in front of an inhomogeneous obstacle composed of a porous medium, the study successfully suppresses reflections and attains high transmittance. While previous research has focused on adjusting wavefronts to enhance transmission efficiency, the investigation of eliminating reflections and achieving total transmission still needs to be improved.

The fabricated design layer optimized through GA optimization with an appropriate cost function demonstrates remarkable efficiency in minimizing reflections by strategically arranging holes at specific locations. The optimized design yields more than double the transmittance compared to existing systems and enables complete transmission in cases previously deemed impossible.

Nevertheless, the system constructed through optimization may exhibit heightened sensitivity to frequency and position errors, warranting further attention. Additionally, the study's scope is limited to achieving anti-reflection for specific distributions with fixed locations, while obstacles with arbitrary distributions still need to be addressed. Consequently, future research endeavors should focus on devising a design layer capable of accommodating obstacles with diverse distributions.

Notwithstanding the need for follow-up studies, the proposed method is expected to contribute to ultrasound examination and

treatment significantly. Its application holds immense potential to advance the practicality and efficacy of ultrasound-based procedures.

Bibliography

[1] C.R. Farrar and K. Worden, “An introduction to structural health monitoring”, Philosophical Transactions of the Royal Society A, 303-315, 2007.

[2] J. L. Rose, “Ultrasonic waves in solid media”, Cambridge University Press, 2004.

[3] P. Burrascano, S. Callegari, A. Montisci, M. Ricci, and M. Versaci, “Ultrasonic nondestructive evaluation systems: industrial application issues”, Springer International Publishing, 2015.

[4] Atsushi Hosokawa, “Development of a Numerical Cancellous Bone Model for Finite-Difference Time-Domain Simulations of Ultrasound Propagation”, IEEE transactions on ultrasonics, ferroelectrics, and frequency control, vol. 55, no. 6, 2008.

[5] Yujiao Guo, Ying Liu, Xingang Wang, Gang Li, Guoxia Yu, “Clinical and imaging features of melanotic neuro ectodermal tumor of infancy of the maxillary bone: report of four cases and review of the literature”, Oral Radiology, 38:630–637, 2022.

[6] Thomas Riis, Taylor Webb, Jan Kubanek, “Acoustic properties across the human skull”, Department of Biomedical Engineering, 84112, 2021.

[7] Leitao Cao, Qiuxia Fu, Yang Si, Bin Ding, Jianyong Yu, “Porous materials for sound absorption”, Composites Communications, 10 25-35, 2018.

[8] Mathias Fink, “Time-reversal acoustics”, Journal of Physics, 118 012001, 2008.

[9] Heekyung Koh, Tae Young Park, Yong An Chung, Jong-Hwan Lee, and Hyungmin Kim, “Acoustic simulation for transcranial focused ultrasound using GAN-based synthetic CT”, IEEE journal of biomedical and health informatics, vol. 26, no. 1,

2022.
[10] Y. Liu and X. Zhang, “Metamaterials: a new frontier of science and technology”, Chemical Society Reviews, 40(5), 2494-2507, 2011.
[11] S. A. Cummer, J.Christensen, and A. Alu, “Controlling sound with acoustic metamaterials”, Nature Reviews Materials, 1(16001), 2016.
[12] H. T. Chen, A. J. Taylor, and N. Yu, “A review of metasurfaces: physics and applications”, Reports on Progress in Physics, 79(7), 076401, 2016.
[13] J. Jung, H. Park, J. Park, T. Chang, and J. Shin, “Broadband metamaterials and metasurfaces: a review from the perspectives of materials and devices”, Nanophotonics, 9(10), 3165-3196, 2020.
[14] Hong Jae Kim, Chung Il Park, Kiyean Kim, and Yoon Young Kim, “Meta-ring for Enhancing Emission Efficiency of Omnidirectional SH Waves,” International Journal of Mechanical Sciences, Vol. 251, 108354 ,2023.
[15] Jeseung Lee, Minwoo Kweun, Woorim Lee, Chung Il Park, and Yoon Young Kim, “Perfect Transmission of Elastic Waves Obliquely Incident at Solid–solid Interfaces,” Extreme Mechanics Letters, Vol. 51, 101606, Feb. 2022.
[16] Shin Young Kim, Yu Bin Oh, Joong Seok Lee, and Yoon Young Kim, “Anomalous Mode-converting Reflection of Elastic Waves Using Strip-type Metagratings,” Mechanical Systems and Signal Processing, Vol. 186, 109867, 2023.
[17] Jeseung Lee, Jooa Park, Chan Wook Park, Seung Hyun Cho, and Yoon Young Kim, “Uni-modal Retroreflection in Multi-modal Elastic Wave Fields,” International Journal of Mechanical Sciences, Vol. 232, 107655, 2022.
[18] Sun, Shulin, et al. "High-efficiency broadband anomalous

reflection by gradient meta-surfaces" Nano letters, 12, 2012.
[19] Chan Wook Park, and Yoon Young Kim, "Theoretical analysis of transmission and phase coverage by a symmetric metasurface across dissimilar media".
[20] Auld, Bertram Alexander, “Acoustic fields and waves in solids”, Рипол Классик, 1973.
[21] Matteo Mazzotti, Eetu Kohtanen, Alper Erturk and Massimo Ruzzene, “Radiation Characteristics of Cranial Leaky Lamb Waves”, IEEE transactions on ultrasonics, ferroelectrics, and frequency control, vol. 68, no. 6, 2021.
[22] Raktim Sarma, Abigail Pribisova, Bjorn Sumner and Jayson Briscoe, “Classification of Intensity Distributions of Transmission Eigenchannels of Disordered Nanophotonic Structures Using Machine Learning”, Appl. Sci, 12, 6642, 2022.
[23] Michael Horodynski, Matthias Kühmayer, Andre Brandstötter, Kevin Pichler, Yan V. Fyodorov, Ulrich Kuhl and Stefan Rotter, “Optimal wave fields for micromanipulation in complex scattering environments”, Nature Photonics, vol. 14, 149–153, 2020.
[24] Lee, Sung Won, et al. "Mode-Selective Elastic Metasurfaces", Physical Review Applied, 19.1(014024), 2023.
[25] Michael Horodynski, Matthias Kühmayer, Clément Ferise, Stefan Rotter and Matthieu Davy, “Anti-reflection structure for perfect transmission through complex media”, Nature, vol. 607, 14, 2022.

초록

불균일한 매질에서의 음파 전송은 의학 분야의 영상 촬영, 치료 및 비파괴 검사와 같은 다양한 초음파 응용 분야에서 중요한 과제입니다. 파면 제어를 사용한 시간 역전(time-reversal) 방법은 특정 영역으로의 에너지 전송을 향상시킬 수 있는 가능성을 보여주었지만 불균일한 매질과 바탕 매질 사이의 고유한 임피던스 불일치를 해결하지 못하여 결과적으로 바람직하지 않은 후방 산란 및 반사가 발생합니다. 이러한 한계를 극복하기 위해 본 논문에서는 불균일한 매질 앞에 잘 설계된 무반사 메타물질을 배치하여 반사 없이 모든 입사 에너지의 전송을 가능하게 하는 새로운 방법론을 제시합니다. 무반사 메타물질은 2D guided wave 시스템에서 단순한 구멍들로 구성된 다공성 층으로 제작되며 이러한 구멍의 위치는 유전 알고리즘(GA)을 사용하여 최적화됩니다. 수치 시뮬레이션을 통해 제작된 메타물질의 성능을 평가한 결과, 메타 물질이 두 가지 다른 시스템, 공기 상에 강체 장애물이 있는 시스템과 물 속에 두개골 장애물이 있는 시스템에서 반사를 효과적으로 억제한다는 것을 확인했습니다. 본 연구에서 제안하는 무반사 메타물질은 복잡한 매체에서 음파 에너지의 전송 효율을 향상시킬 수 있는 방법을 제공하여 다양한 영역에서 초음파 응용 분야의 발전에 크게 기여할 것으로 기대됩니다.

주요어 : 음파, 반사 방지, 메타물질, 불균일한 매질, 완전 투과, 다공정 매질

학 번 : 2021-25481